American Genetic Association

Journal of Heredity, 2020, 1–15
doi:10.1093/jhered/esaa015
Original Article
Advance Access publication June 1 2020

OXFORD

Original Article

The Genetic Architecture of Plant Defense Trade-offs in a Common Monkeyflower

Nicholas J. Kooyers, Abigail Donofrio, Benjamin K. Blackman, and Liza M. Holeski

From the Department of Biology, University of Louisiana, Lafayette, LA 70503 (Kooyers); Department of Integrative Biology, University of South Florida, Tampa, FL 33620 (Kooyers and Donofrio); Department of Plant and Microbial Biology, University of California, Berkeley, CA 94720 (Blackman); and Department of Biological Sciences, Northern Arizona University, Flagstaff, AZ 86011 (Holeski)

Address correspondence to N. J. Kooyers at the address above, or e-mail: nkooyers@gmail.com

Received March 11, 2020; First decision May 12, 2020; Accepted May 25, 2020.

Corresponding Editor: Scott Hodges

Abstract

Determining how adaptive combinations of traits arose requires understanding the prevalence and scope of genetic constraints. Frequently observed phenotypic correlations between plant growth, defenses, and/or reproductive timing have led researchers to suggest that pleiotropy or strong genetic linkage between variants affecting independent traits is pervasive. Alternatively, these correlations could arise via independent mutations in different genes for each trait and extensive correlational selection. Here we evaluate these alternatives by conducting a quantitative trait loci (QTL) mapping experiment involving a cross between 2 populations of common monkeyflower (*Mimulus guttatus*) that differ in growth rate as well as total concentration and arsenal composition of plant defense compounds, phenylpropanoid glycosides (PPGs). We find no evidence that pleiotropy underlies correlations between defense and growth rate. However, there is a strong genetic correlation between levels of total PPGs and flowering time that is largely attributable to a single shared QTL. While this result suggests a role for pleiotropy/close linkage, several other QTLs also contribute to variation in total PPGs. Additionally, divergent PPG arsenals are influenced by a number of smaller-effect QTLs that each underlie variation in 1 or 2 PPGs. This result indicates that chemical defense arsenals can be finely adapted to biotic environments despite sharing a common biochemical precursor. Together, our results show correlations between defense and life-history traits are influenced by pleiotropy or genetic linkage, but genetic constraints may have limited impact on future evolutionary responses, as a substantial proportion of variation in each trait is controlled by independent loci.

Subject area: Genomics and gene mapping, Quantitative genetics and Mendelian inheritance
Keywords: *Mimulus guttatus* (common yellow monkeyflower), *Erythranthe guttata*, flowering time, plant functional strategies, phenylpropanoid glycosides, quantitative trait loci (QTL)

A commonly observed property of phenotypic diversity is that many traits tend to covary across individuals of a species creating complex multivariate phenotypes. Such phenotypic correlations may arise because certain combinations of traits are advantageous in specific environments (correlational selection; Brodie 1992; McGlothlin et al. 2005) or because developmental or genetic constraints prevent

independent evolution of each trait (Lande 1979; Arnold 1992; Gardner and Latta 2007). At the genomic level, genetic constraints can arise via pleiotropy, the ability of allelic variation in one gene to affect multiple phenotypes, or via genetic linkage that greatly reduces the independent assortment of alleles at linked loci affecting individual traits. The importance of pleiotropy or close linkage relative to correlational selection in creating phenotypic correlations is contentious (Gardner and Latta 2007; Stearns 2010; Paaby and Rockman 2013), but has important consequences for evolutionary responses of populations. That is, pleiotropy or linkage can either facilitate evolution by maintaining adaptive combinations of traits during the evolutionary process (e.g., Lowry and Willis 2010) or constrain evolution by limiting the achievable phenotypic parameter space, altering most likely evolutionary paths, or reducing the speed with which multiple traits keep pace in tracking fitness optima (Etterson and Shaw 2001; McKay et al. 2003). Thus, understanding how quickly and optimally populations are able to adapt to a particular environment depends on understanding the degree and direction of pleiotropy or linkage in ecologically important traits.

One place where genetic correlations caused by pleiotropy or linkage are likely to be important is in the evolution of growth, reproductive timing, and defense strategies in plants. Trade-offs between plant defense and growth or reproduction arise because the allocation of resources to defense involves investment in the synthesis of costly biochemical compounds or physical defenses that may come at the expense of allocating resources to growth and reproduction (Herms and Mattson 1992; Strauss et al. 2002; Stamp 2003). Indeed, genetic covariation between growth or reproduction and constitutive levels of chemical defenses have been frequently observed both within and among populations grown in common garden environments (Koricheva 2002; Kooyers et al. 2017; Defossez et al. 2018; Lowry et al. 2019). The presence of these correlations suggests that either pleiotropic or linked variation underlies differences in resource allocation or that past correlational selection may have independently selected combinations of genotypes at unlinked loci that independently control variation in plant defense, growth, or reproductive rate.

Pleiotropy or linkage are also likely to be important factors in shaping the evolution of plant chemical defense arsenals, which warrant consideration as complex multivariate traits in and of themselves. Plants can produce an immense variety of secondary metabolites for defense against herbivores and pathogens, and individual species frequently produce multiple structurally similar compounds derived from a single biosynthetic pathway (Fraenkel 1959; Keefover-Ring et al. 2014; Raguso et al. 2015). Because these compounds share a biochemical precursor, their individual and relative production levels are largely expected to covary (Berenbaum and Zangerl 1988). However, variation in arsenal composition between populations is common within species (Holeski et al. 2012, 2013; Moore et al. 2014), and observations of covariation between multivariate defenses and fitness, sometimes even in response to site-specific herbivore communities, suggest that such variability in chemical arsenals is often adaptive (Berenbaum and Zangerl 1998; Koricheva et al. 2004; Carmona et al. 2011; Prasad et al. 2012). Pleiotropy or linkage could affect the evolution of defense arsenals in 2 ways. First, a single locus could be positively associated with some defenses, but negatively associated with others, reflecting potential allocation trade-offs. Second, a single locus could be positively associated with multiple defenses (positive pleiotropy) reflecting total carbon allocated to defense rather than other functional traits. Alternatively, pleiotropy or linkage may not come into play, and some loci may only influence variation in production of a single defense compound. Such modular genetic variants would be unconstrained by genetic correlations and allow selection to freely fine-tune defense arsenals to herbivore communities.

Here we examine the genetic architecture of phenotypic correlations between growth, reproductive rate, and the total abundance and composition of chemical defenses in the ecological genetic model plant, *Mimulus guttatus*. Distributed from Mexico to Alaska across a broad range of ecological conditions, *M. guttatus* populations possess exceptionally high levels of genetic diversity and also exhibit tremendous diversity in morphology, phenology, and chemical and physical defense (Holeski 2007; Wu et al. 2008; Flagel et al. 2014; Friedman et al. 2015; Puzey et al. 2017). Across this range, annual populations of *M. guttatus* inhabit sites that differ dramatically in the yearly timing and duration of the growing season. These habitats include seeps, thin-soiled meadows, and rock walls with ephemeral water supplies where the local growing season is defined by the relative timing of spring rains or snow melt and summer terminal droughts. Thus, optimal phenological timing appears to be a critical determinant of fitness in this species, and consequently, spatially and temporally variability in the growing season maintains variation in phenological timing within and between populations (Hall and Willis 2006; Mojica et al. 2012; Kooyers et al. 2015; Monnahan and Kelly 2017; Troth et al. 2018; Nelson et al. 2019).

Differences in allocation of resources to chemical defense are another key axis of variation in the evolution of adaptive strategies in *M. guttatus*. Annual *M. guttatus* populations invest between 3.4% and 37.1% of dry leaf mass to defending their young leaves with diverse arsenals of phenylpropanoid glycosides, or PPGs (Holeski et al. 2013; Keefover-Ring et al. 2014; Kooyers et al. 2017). PPGs are synthesized via the shikimic acid pathway and have been documented as generalist herbivore feeding deterrents and specialist feeding stimulants in several plant species, including *M. guttatus* (Molgaard 1986; Holeski et al. 2013, 2014; Rotter et al. 2018). A previous range-wide population survey of >30 annual *M. guttatus* populations detected dramatic among-population differentiation in the total constitutive level of PPGs and in the compositions of PPG arsenals (Kooyers et al. 2017). Variation in defense compound abundance is strongly correlated with variation in both growing season length and flowering time suggesting that there are trade-offs between chemical defenses and reproductive timing that underlie adaptation among populations. Whether these trade-offs are caused by genetic correlations or correlational selection is unknown, but could profoundly impact how these populations respond to changing climates (Kooyers et al. 2019).

In this study, we take a quantitative trait locus (QTL) mapping approach to ask whether loci that influence variation in growth, reproduction, constitutive chemical defense levels, and individual defense metabolite abundances colocalize; thus, testing whether phenotypic correlations among combinations of these phenotypes could be caused by pleiotropy or close linkage. Leveraging a cross derived from California and Oregon parents distinguished by divergent growth rates, constitutive PPGs levels, and PPG arsenal compositions, we characterize the genetic architecture underlying this variation to investigate the following 3 questions. First, do the genetic correlations between traits in this F_2 mapping population parallel the phenotypic correlations observed among parents and/or wild populations? Second, do QTLs underlying variation in growth rate, reproductive rate, and constitutive PPGs colocalize? Finally, do QTLs underlying variation in individual PPG levels reflect "defense" loci where one allele is associated with increases in levels of all

PPGs, do they reflect "allocation" loci where one allele is associated with increases in levels of some PPGs but not others, or do different PPGs have entirely independent QTLs? Together, our analyses suggest that trade-offs between growth, defense, and reproduction reflect the combined influence of genetic correlations and correlational selection.

Methods

An F_2 mapping population was generated from an initial cross between a parental line from a low elevation inland annual population found north of Fresno, CA (BEL: 37.039833, −119.77382; elevation = 188 m) and a parental line from a high elevation annual population found on Iron Mountain, OR (IM62: 44.402389, −122.15325; elevation = 1358 m) followed by selfing of a single F_1 plant. For simplicity, we refer to these lines as the CA and OR parental lines below. Parental lines were inbred via single seed descent for multiple generations prior to generating the mapping population (CA: 2 generations, OR: >5 generations). The parent lines for this cross were chosen because they differed dramatically in PPG arsenal, PPG total level, and growth rate under common garden greenhouse conditions (Kooyers et al. 2017).

Plant Growth and Experimental Design

We conducted a QTL mapping experiment using the above lines in a walk-in environmental chamber at the University of South Florida (Environmental Growth Chambers custom model). Parental, F_1, and F_2 seeds were sown in Fafard 3b potting media (Sun Gro Horticulture; Agawam, MA) in 2.5" square pots within 1020 flats with humidity domes and stratified at 4 °C for 7 days. Flats were then moved to the growth chamber, and germination occurred under humidity domes for 7 days. Seedlings were thinned to 1 plant in each pot (16 CA parental lines, 10 OR parental lines, 21 F_1, and 400 F_2 plants germinated). Plants were raised in the growth chamber under 16 h day:8 h night cycles at a constant temperature of 18 °C, bottom-watered as necessary, and rotated every 2–3 days to minimize fine-scale spatial effects. No supplemental fertilizer was applied until after all phenotypes were collected. This chamber had never been previously used to grow plants, and we observed no evidence of herbivory during the experiment.

We scored each plant for a suite of morphological, phenological, and plant defense phenotypes. Germination and flowering status were surveyed daily to quantify flowering time as the number of days between the germination date and day of first flower. On the day of first flower, we recorded several growth traits including plant height, flowering node, branch number, and leaf width and leaf length of the larger second true leaf. Growth rate before flowering was calculated as plant height divided by flowering time. At flowering, we also removed a single second true leaf, dried it at 65 °C for 4 days before weighing to obtain dry leaf weight. Because most morphological phenotypes were highly correlated and the results from each were repetitive, we report only plant height in the main text and report results from a supplementary principal component analysis (PCA) on morphological phenotypes in Supplementary Table S1. Previous studies have shown strong correlations between total above grown biomass and plant height (Rotter et al. 2019). Sampling for phytochemical analysis consisted of flash freezing the other second true leaf as well as the third and fourth true leaves in liquid nitrogen after full expansion of the fifth true leaves. All leaf material was freeze-dried using a pre-chilled Freezemobile freeze drier system (SP Scientific FM25XL-70). Nearly all plants had flowered prior to tissue collection for phytochemical analyses. Following phenotyping, floral buds were collected for DNA extraction and downstream genetic analysis.

Extraction of PPGs and analysis of quantitative PPG content via high-performance liquid chromatography followed previously established procedures (Holeski et al. 2013, 2014; Kooyers et al. 2017). PPG quantities were calculated as verbascoside equivalents using a standard solution of pure verbascoside as in Holeski et al. (2013). Our methods were not fully robust for samples with less than 3 mg of freeze-dried tissue; therefore, we excluded apparent outlier samples. We also excluded a single individual from the California parent line that was an outlier for nearly all phenotypes. Because its pot was adjacent to several OR parental line individuals in the experiment, we suspect an OR plant that somehow made it into this pot on accident.

Summary statistics including mean, standard deviation, and standard error were calculated for all growth, flowering time, and PPG phenotypes. We assessed differences among parent lines with Welch 2 sample *t*-tests assuming equal variance. To determine whether genetic correlations exist between chemical defenses and growth rate, reproductive rate, or trichome density, we calculated Pearson correlations between total PPGs and growth rate, as well as between total PPGs and flowering time in the F_2 population. We also assessed Pearson correlations between constitutive production of different PPGs to examine whether different PPGs were genetically correlated. Because we observed extensive correlations in the abundances of different PPGs, we conducted a PCA with imputation of missing phenotypes via the *pcaMethods* package version 1.74 (Stacklies et al. 2007) to summarize variation in PPG arsenals. Traits were *z*-score transformed prior to the PCA.

Genotyping and QTL Mapping

We extracted DNA from buds sampled from each plant using a modified CTAB extraction procedure (Kelly and Willis 1998). DNA was quantified using a fluorescent plate reader (Molecular Devices Gemini XS Plate Reader) and Quant-iT dsDNA broad-range assay kits (ThermoFisher Scientific; Waltham, MA). Plants were genotyped via a custom multiplex shotgun genotyping procedure (Andolfatto et al. 2011; Ferris et al. 2017). Briefly, we performed an AseI (NEB; Ipswich, MA) restriction digest on input 50-ng DNA from each sample. One of 40 custom-barcoded adaptors was ligated onto each sample, and groups of products with unique barcodes were pooled. We size selected each of the 10 resulting pools using a PippenHT instrument (Sage Science, Beverly, MA). Each pool was then amplified with a primer set containing a unique index (initial denaturation: 30 s at 98 °C; amplification: 10 s at 98 °C, 15 s at 60 °C, and 15 s at 72 °C for 16 cycles; final extension: 7 min at 72 °C). Thus, each sample could be distinguished by a unique adaptor barcode: sequencing index combination. Indexed libraries were combined in normalized pools and sequenced on a single lane of Illumina HiSeqX (paired-end, 150 bp reads; Novogene; Sacramento, CA).

We used TASSEL 5 GBS V2 pipeline for identification of SNPs, SNP calling, and quality filtering (Glaubitz et al. 2014). Alignment of tags to the *M. guttatus* reference genome v2.0 (Hellsten et al. 2013) was performed with Bowtie2 v2.3.2 (Langmead and Salzberg 2012) with the very sensitive option. Potential SNPs were discarded if minor allele frequency was <10%, if the minor allele appeared was not homozygous in 1% of individuals, or if the minor allele did not appear in >10% of depth at a locus. We also discarded all SNPs

that did not map to scaffolds 1–14 (corresponding to chromosomes 1–14). This data were further filtered to exclude any individuals that had SNPs called for <25% sites and to include only sites where CA and OR parent were homozygous for alternative alleles. A custom perl script was used to create genotype calls for 40-SNP wide windows across the genome resulting in 683 windows. This method produced an excess of heterozygotes relative to homozygotes for most window-based markers.

We used the scripts documented in GOOGA for calculating error rates, filtering individuals, producing a linkage map, and calculating genotype probabilities (Flagel et al. 2019). Three different measures of genotyping error rate were calculated for every individual: error due to the probability that a homozygote is mistakenly called a heterozygote, the probability that a homozygote is mistakenly called the alternative homozygote, and the probability that a true heterozygote is called either homozygote. Individuals with greater than 20% error in any of these categories were dropped from linkage map creation. Linkage maps were generated with the remaining individuals (N = 113). Any window-based markers with the maximum recombination distance between them were dropped from the analysis (12 markers dropped), and both the error rate analysis and linkage map construction were rerun without these markers. This process decreased linkage map size to 1614 cM, similar to other linkage maps constructed for *M. guttatus* (Flagel et al. 2019). Using these errors rates and linkage maps, we assessed genotype posterior probabilities for each marker for each individual including those previously dropped from the linkage map construction. Any genotype calls with posterior probability under 90% were designated as missing data.

The rQTL v1.41–6 package (Broman et al. 2003) was used to perform single- and multiple-locus QTL mapping. The data set used for interval mapping consisted of 241 F_2 individuals and 671 markers. Genotyping coverage was 94% and phenotype coverage ranged from 81% to 100% depending on phenotype. Thus, the number of observations used in QTL analysis ranges from 194 to 234 individuals (Supplementary Table S2). Conditional genotype probabilities were calculated based on a genotyping error rate of 1% and a step of 1 cM. To detect single QTLs, the scanone function with the EM algorithm was used (Lander and Botstein 1989). Using the same function with the Haley–Knott regression in rQTL produced nearly identical results (Haley and Knott 1992). We used a permutation test (randomly assigning phenotypes to different genotypes) to determine an appropriate significance threshold for QTLs. We report the 10%-LOD permutation thresholds below, but nearly all QTLs surpass the 5% thresholds as well. Additive ($a = (\mu_{BB} - \mu_{AA})/2$) and dominance ($d = \mu_{AB} - (\mu_{AA} + \mu_{BB})/2$) effects of each QTL were estimated via genotype means for the marker nearest the estimated center of the QTL. To estimate the variance associated with each individual QTL as well as all QTLs detected for a phenotype, we created multiple QTL models. We first created multiple QTL models for each trait using the makeqtl function including all QTLs detected by the single-locus models as additive variables. We then summarize the variance associated with each QTL using the fitqtl function. We also constructed models that include epistatic interactions when multiple QTLs were detected for a trait, but these models were probably underpowered as our data set contained only 241 individuals.

To assess the role of pleiotropy or close genetic linkage in producing phenotypic and genetic correlations, we examined colocalization between QTLs for different traits. We determined that 2 QTLs for different traits colocalized when their 1.5-LOD support intervals overlapped. To determine the multitrait influence of each shared QTL, we examined the allelic effects on each phenotype and compared the direction of these effects to divergence between parental lines.

Results

Ample Phenotypic Divergence Between Parental, F_1, and F_2 Plants

Parental lines from California and Oregon differed significantly in morphology, growth rate, and total PPG levels (Table 1; Figure 1). The CA parental line had lower levels of total PPG production, was taller at flowering, and had a higher growth rate prior to flowering than the OR parental line (Table 1; Figure 1A,C,D). Parental plants did not differ significantly in flowering time. Both parental lines flower rapidly in permissive day lengths compared with other annual *M. guttatus* populations throughout the range (Figure 1B), but notably, they differ in how they manifest early flowering. CA parental line plants grow and add new nodes rapidly prior to flowering while OR parental line plants flower do not accelerate vegetative growth and accumulate fewer nodes prior to flowering than CA (Kooyers

Table 1. Summary statistics for parental, F_1 and F_2 accessions

Trait	CA	OR	F_1	F_2	Student's t	P
	Mean (SD)	Mean (SD)	Mean (SD)	Mean (SD)		
Ability to flower	0.733	0.6	0.57	0.838	—	0.67
Flowering time	25.2 (2.82)	28.67 (5.79)	33 (7.82)	32.19 (7.33)	1.63	0.127
Plant height	7.07 (2.7)	2.8 (0.76)	3.94 (1.15)	5.64 (2.45)	−3.35	0.005
Growth rate	0.29 (0.11)	0.1 (0.03)	0.13 (0.05)	0.18 (0.08)	3.34	0.005
Unknown PPG 10	0.41 (0.17)	0.15 (0.06)	0.34 (0.08)	0.31 (0.14)	−3.21	0.007
Calceolarioside A	23.59 (4.73)	11.06 (1.55)	23.9 (6.58)	20.61 (8)	−5.68	<0.001
Conandroside	34.03 (11.38)	53.24 (12.29)	72.52 (20.25)	56.63 (36.37)	3.01	0.010
Verbascoside	3.37 (1.09)	1.93 (0.47)	3.65 (1.27)	3.2 (2.56)	−2.78	0.016
Calceolarioside B	0.25 (0.08)	0.47 (0.29)	0.51 (0.2)	0.39 (0.3)	2.22	0.045
Mimuloside	0.91 (0.39)	3.25 (0.39)	2.31 (0.71)	1.98 (1.62)	11.02	<0.001
Unknown PPG 16	3.95 (1.32)	11.93 (3.18)	6.21 (2.09)	4.39 (3.68)	7.02	<0.001
Total PPGs	66.51 (8.93)	82.03 (9.63)	109.45 (20.95)	87.23 (41.25)	3.10	0.009

Ability to flower is the proportion of plants that flowered during the experiment. Student's t and P-value correspond to a Welch's t-test, assessing significant differences between parental lines. All Welch's t-tests had 13 degrees of freedom except for plant height, which had 14 degrees of freedom. Statistics examining differences in the ability to flower between parental lines are Fisher's exact tests rather than t-tests.

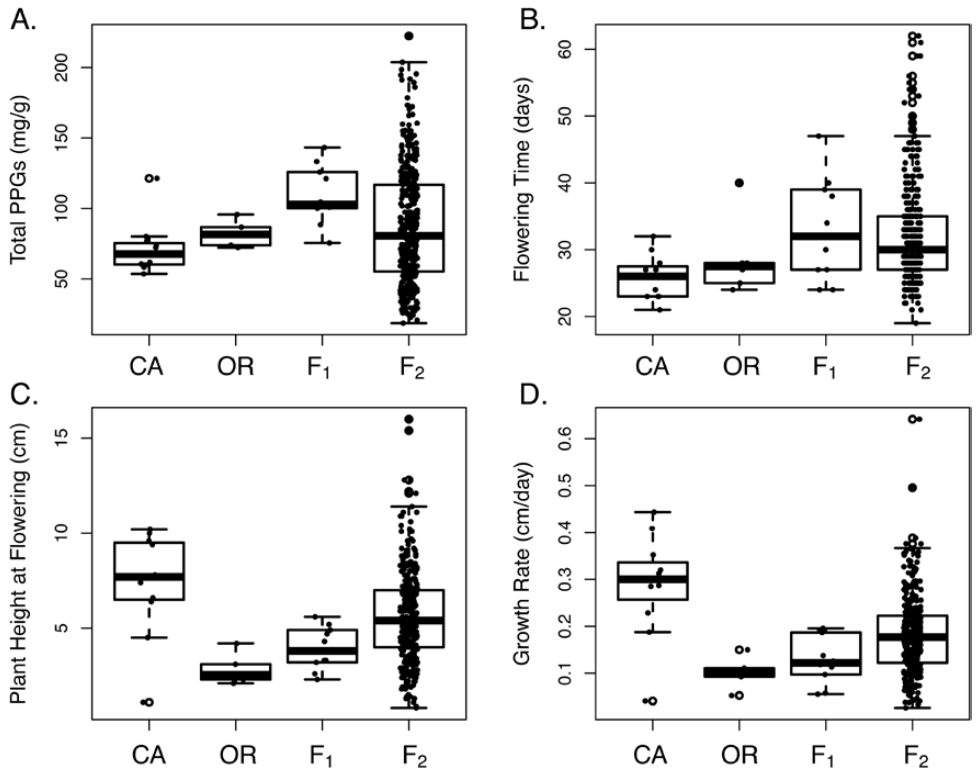

Figure 1. Variation in California (CA) and Oregon (OR) parental lines, F_1 individuals, and F_2 mapping population for (**A**) total PPGs, (**B**) flowering time, (**C**) plant height at flowering, and (**D**) growth rate prior to flowering. In each boxplot, the bottom and top of the box represent first and third quartiles and the center line is the median. Whiskers represent the less extreme value of either the minimum/maximum value or 1.5 times the interquartile range.

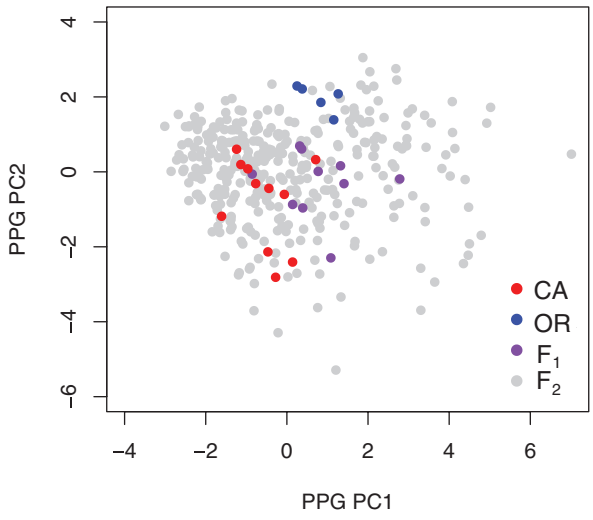

Figure 2. Principal component analysis of PPG arsenals for CA parents, OR parents, F_1 lines, and F_2 lines. The PPG PC1 axis (41.6% of variation) loads on all PPGs where higher levels are correlated with greater amounts of all PPGs beside calceolarioside A. The PPG PC2 axis (24.0% of variation) loads on calceolarioside A and unknown PPG 10 where lower values correspond to greater levels of both of these PPGs.

et al. 2015, 2019). PPG arsenals also differed between parental lines (Figure 2; Supplementary Figure S1). The California parental line produced higher constitutive levels of calceolarioside A, unknown PPG 10, and verbascoside, whereas the Oregon parental line produced higher constitutive levels of conandroside, calceolarioside B, mimuloside, and unknown PPG 16 (Table 1).

Patterns of trait variation in the F_1 and F_2 plants varied greatly among traits. F_1 plants produced higher constitutive total levels of PPGs and flowered later on average than either parental line, and this overdominant trait expression may indicate heterotic effects or transgressive segregation (Figure 1; Table 1). The mean growth rate for the F_1 plants was intermediate to the parental line means but somewhat closer to the Oregon parent line mean, suggesting incomplete dominance (Figure 1). Different PPGs exhibited different patterns of dominance (Supplementary Figure S1). The average concentration of calceolarioside B in F_1 plants was similar to the OR parental line, whereas the average concentrations of calceolarioside A, verbascoside, and unknown 10 were similar to the CA parental line. Concentrations of conandroside in the F_1 plants exceeded either parent, and concentrations of unknown PPG 16 and mimuloside were intermediate to the parents. For every trait surveyed, F_2 populations were highly variable, often exceeding the minimum and maximum trait values for the parental and F_1 lines, and thus indicative of transgressive segregation (e.g., Figure 1). The F_2 trait means for all traits except flowering time and conandroside were intermediate to the parental line means (Table 1; Supplementary Figure S1).

Genetic Correlations Often but Not Always Align With Parental Trait Differences

Genetic correlations between traits in the F_2 generation generally paralleled the phenotypic divergence observed between the parental lines. For instance, total levels of PPGs were moderately correlated with flowering time where plants that produced lower total PPG

levels typically flowered earlier (r^2 = 0.35; Figure 3A; Table 2), consistent with phenotypic correlations and suggestive of a trade-off between these traits observed among annual populations range-wide (Kooyers et al. 2017). However, genetic correlations between total PPG level and plant height (r^2 = 0.003; Figure 3B) or growth rate (r^2 = 0.10; Figure 3C) were absent or weak, respectively, suggesting that parental divergence for these phenotypes probably arose via changes at independent genetic loci.

Patterns of covariation among different PPGs in the F_2 panel closely mirrored the differences that we observed between the parent lines and observed in past population surveys (Kooyers et al. 2017). There are strong correlations between conandroside, calceolarioside B, unknown PPG 16, mimuloside, and verbascoside (0.38 < r < 0.73; Table 2). Together these PPGs make up a single principal component axis (PPG PC1; 46.2% of variance) where larger values of PC1 are associated with greater concentrations of each compound. The concentration of unknown PPG 10 is moderately correlated with the above PPGs (0.24 < r < 0.41) and with PPG PC1 (Supplementary Table S3). However, it is more strongly correlated with calceolarioside A (r = 0.67, P < 0.0001), and these 2 PPGs load strongly on a second principal component axis (PPG PC2; 24% of variance) with higher concentrations of each PPG associated with lower PPG PC2 scores. Calceolarioside A is weakly or negatively correlated with all other PPGs. The similarity of the PCA in the present study to the PCA in our previous population survey (Kooyers et al. 2017) suggests that the 2 parents used here may adequately represent the genetic constraints across the range (Supplementary Table S3).

A Single QTL Explains Variation in Both Flowering Time and Total PPGs

As with the genetic correlations, results from QTL analyses support the role for pleiotropy or close linkage accounting for some of the phenotypic correlations among parental plants. We detected QTLs for total PPG concentration on chromosomes (chr.) 1, 10, 13, and 14 (Table 3; Figure 4) whose additive effects together accounted for 32% of the total variation in total PPG levels. When epistatic interactions between QTLs are incorporated into this model, these 4 QTLs account for up to 60% of variation in total PPGs (Supplementary Tables S4 and S5). The directions of QTL effects were consistent with the polarity of the parental line differences, i.e. constitutive PPG levels increased with the number of OR alleles an individual carried at each QTL. Although no flowering time QTLs were detected at our chosen LOD score threshold, one QTL very close to meeting that threshold (LOD = 2.98 vs. 3.29) colocalized with the QTL for total PPG level on chr. 10 (Table 3; Figure 4). Plants with more OR alleles at this QTL flowered later and had higher total PPG concentrations (Figure 5). Given that our mapping panel sampled a limited number of recombination events, the 1.5 LOD support intervals surrounding these QTLs are broad (ranging from 6.9 to 17 million bp) and lack the resolution to distinguish whether pleiotropy or linkage is the mechanism that explains the covariation of flowering time and concentration of total PPGs accounted for by this region.

A nontrivial portion of the F_2 mapping panel never flowered (28 of 241), and we detected a single minor effect QTL on chr. 14 that explained variation whether or not plants flowered in our experiment (Figure 6). Although this QTL does not colocalize with the total PPG QTL on chr. 14, allelic variation does significantly correlate with both phenotypes at best estimate markers for each QTL. No QTLs associated with variation in growth rate or plant height at flowering were detected, suggesting variation in these traits is probably highly polygenic. The marker with the highest LOD score for both growth rate and plant height at flowering was on chr. 8 and did not colocalize with any other QTLs in the study. Taken together these results suggest that both pleiotropy and close linkage play some role in shaping phenotypic correlations between reproductive timing and chemical defense production.

Divergent PPG Arsenals Are Largely Controlled by Independently Segregating QTLs

Our QTL analyses detected sets of loci that explained variation in the concentrations of most individual PPGs, and there was colocalization for several QTLs found for different PPGs. One to 6 QTLs explained variation in each individual PPG level; single locus QTL models explained 6–22% of variation; and additive multiple locus models explained 9.8–43.7% of variation. The only exception was for calceolarioside B, for which no QTLs were detected that exceeded the significance threshold. For conandroside and mimuloside, we detected QTLs located in the same region of chr. 10 that explains variation in both flowering time and total PPG levels (Table 3; Figure 5). Plants with more CA alleles have lower levels of each of these PPGs on average. QTLs for several PPGs—including conandroside, verbascoside, unknown PPG 10, and unknown PPG 16—had overlapping 1.5 LOD support intervals on chr. 13 (Table 3; Figure 7), and this region also overlapped with a QTL for total PPGs. Another set of PPGs (conandroside, calceolarioside A, and unknown PPG 10) have individual QTLs with overlapping 1.5 LOD

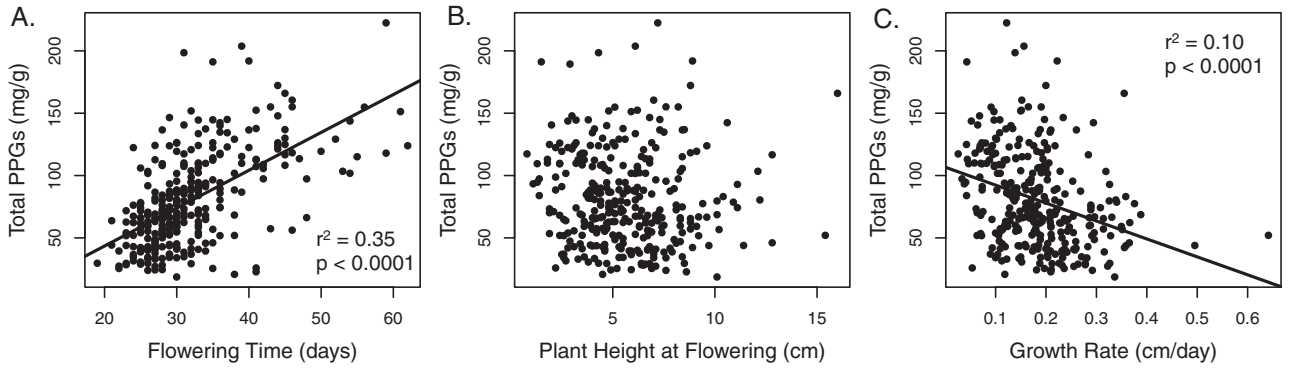

Figure 3. Genetic correlations between of growth and reproductive timing with chemical defense allocation. Scatterplots depict relationships between constitutive total PPG concentrations and (**A**) flowering time, (**B**) plant height at flowering, and (**C**) growth rate prior to flowering. Each point represents a single individual in the F_2 mapping population.

Table 2. Genetic correlations between phenylpropanoid glycosides

	Flowering time	Plant height	Unk. PPG 10	Calc. A	Conand.	Verb.	Calc. B	Mimul.	Unk. PPG 16	Total PPGs
Flowering time		0.072	**0.004**	**0.005**	**>0.001**	**>0.001**	**>0.001**	**>0.001**	**>0.001**	**>0.001**
Plant height	0.1		0.919	0.192	0.214	0.689	0.430	0.474	0.018	0.325
Unk. PPG 10	**0.16**	−0.01		**>0.001**	**>0.001**	**>0.001**	**>0.001**	**>0.001**	**>0.001**	**>0.001**
Calc. A	**−0.16**	0.07	**0.67**		0.060	0.052	0.259	**0.001**	0.030	0.104
Conand.	**0.62**	−0.07	**0.25**	−0.1		**>0.001**	**>0.001**	**>0.001**	**>0.001**	**>0.001**
Verb.	**0.38**	0.02	**0.41**	−0.1	**0.52**		**>0.001**	**>0.001**	**>0.001**	**>0.001**
Calc. B	**0.41**	−0.05	**0.25**	−0.06	**0.6**	**0.57**		**>0.001**	**>0.001**	**>0.001**
Mimul.	**0.54**	−0.04	**0.24**	**−0.17**	**0.73**	**0.44**	**0.4**		**>0.001**	**>0.001**
Unk. PPG 16	**0.46**	−0.14	**0.3**	−0.12	**0.59**	**0.44**	**0.38**	**0.59**		**>0.001**
Total PPGs	**0.59**	−0.06	**0.41**	0.09	**0.98**	**0.56**	**0.61**	**0.73**	**0.64**	

Pearson correlations are found below the diagonal, while *P*-values are found above the diagonal. Bold values indicate statistical significance at $P < 0.01$. Calc. A, Calceolarioside A; Calc. B, Calceolarioside B; Conand., Conandroside ; Verb., Verbascoside; Mimul., Mimuloside.

Table 3. Description of QTL position, percent variance explained, and additive/dominance effects for all traits

Phenotype	Chr	pos (cM)	LOD	PVE (r^2)	Low estimate (bp)	Peak estimate (bp)	High estimate (bp)	*a*	*d*	Degree of dominance
Ability to flower	14	93.3	3.91	0.09	16 476 214	21 044 473	23 055 805	0.15	0.09	0.63
Flowering time[a]	10	20	2.97	0.06	833 345	1 662 700	7 744 804	3.36	1.82	0.54
	11	53.6	2.9	0.06	5 246 106	5 465 507	13 500 702	0.57	4.95	8.63
Growth rate[a]	8	116	3.03	0.07	250 460	16 809 793	21 293 147	0.04	0.02	0.56
Total PPGs	1	78.7	4.54	0.04	7 023 196	12 888 609	12 888 609	11.66	24.84	2.13
	10	47.1	4.75	0.04	833 345	16 390 815	17 879 741	13.55	7.38	0.54
	13	44	7.37	0.06	7 238 546	10 848 557	13 111 267	17.79	14.64	0.82
	14	68.2	6.14	0.09	8 500 856	14 297 905	15 366 375	17.49	5.11	0.29
Calceolarioside A	4	81.1	5.99	0.09	5 152 877	13 656 532	14 771 636	4.49	0.56	0.12
	14	89.3	4.21	0.06	7 653 586	20 677 142	22 471 653	2.82	0.75	0.26
Conandroside	1	78.7	4.61	0.04	7 023 196	12 888 609	12 888 609	11.29	22.33	1.98
	7	29	3.86	0.07	740 073	3 022 495	4 858 091	13.88	6.38	0.46
	10	47.1	4.57	0.04	833 345	16 390 815	17 879 741	12.37	4.55	0.37
	11	32	4.21	0.08	1 487 823	2 681 614	15 544 490	15.50	2.84	0.18
	13	44	6.39	0.05	7238546	15 424 857	13 111 267	14.26	11.46	0.80
	14	68.2	4.52	0.07	8 500 856	14 297 905	15 366 375	14.23	4.64	0.33
Verbascoside	13	40	5.6	0.10	7 238 546	7 692 903	13 111 267	0.96	0.90	0.94
Unknown PPG 10	3	7.21	3.42	0.06	388 849	3 619 813	15 750 736	0.06	0.02	0.27
	13	74.65	3.76	0.05	715 805	15 912 621	26 451 320	0.05	0.00	0.03
	14	59	4.31	0.06	7 399 949	8 500 856	21 721 424	0.04	0.02	0.39
Mimuloside	10	21	10.81	0.22	1 175 820	1 662 700	7 7448 04	1.33	0.96	0.72
Unknown PPG 16	13	41.3	4.8	0.10	7 238 546	9 981 252	16 681 094	2.07	1.52	0.74

Abbreviations for chromosome (chr) and peak position on the genetic map (pos) are used. Estimates refer to the center window position of the closest loci to low, peak, or high 1.5-LOD support intervals. Parameters r^2, *a*, and *d* are calculated from makeqtl models where best estimates of peaks are used to construct multiple QTL models for each trait.

[a]A particular QTL did not meet the LOD threshold for statistical significance.

support intervals on chr. 14 (Table 3; Figure 6). On both chr. 13 and chr. 14, CA alleles are associated with lower levels of each of these PPGs (Figures 6 and 7) and both colocalize with total PPG QTLs.

There are also several QTLs associated with constitutive production of just a single PPG. For instance, QTLs for conandroside occur on chr. 1, chr. 7, and chr. 11 (Figure 7). Notably, OR alleles are associated with higher production of this defense compound for the QTLs on chr. 1 and chr. 7, but CA alleles are associated with higher defense production for the QTL on chr. 11. There are additional QTLs for unknown PPG 10 on chr. 3 and for calceolarioside A on chr. 4 (Figure 7). For each of these QTLs, plants with CA alleles had higher levels of each PPG. These compound-specific QTLs accounted for similar amounts of variation as the multicompound QTLs above (7%–14%, average = 10.6%), although allelic effects at each of these did not necessarily match expectations from the parental lines (Tables 1 and 3).

Discussion

Patterns of correlated differentiation of multiple traits among populations may reflect evolution either constrained by pleiotropy or close physical linkage of variants affecting each trait or through the assembly of allelic variation at multiple unlinked loci into co-adapted genotypes. Our analyses reveal genetic architectures that are consistent with both these possible explanations for explaining correlations between growth, reproductive timing, and defense traits in annual populations of the common monkeyflower, *M. guttatus*. The 2 parental lines for our F_2 mapping panel differed substantially in total levels of chemical defense (PPGs), chemical defense arsenal, and growth rate, reflective of joint patterns of divergence observed across populations in a previous study (Table 1; Figures 1 and 2; Kooyers et al. 2017). We observed strong genetic correlations between total concentration of PPGs and reproductive timing as well as between

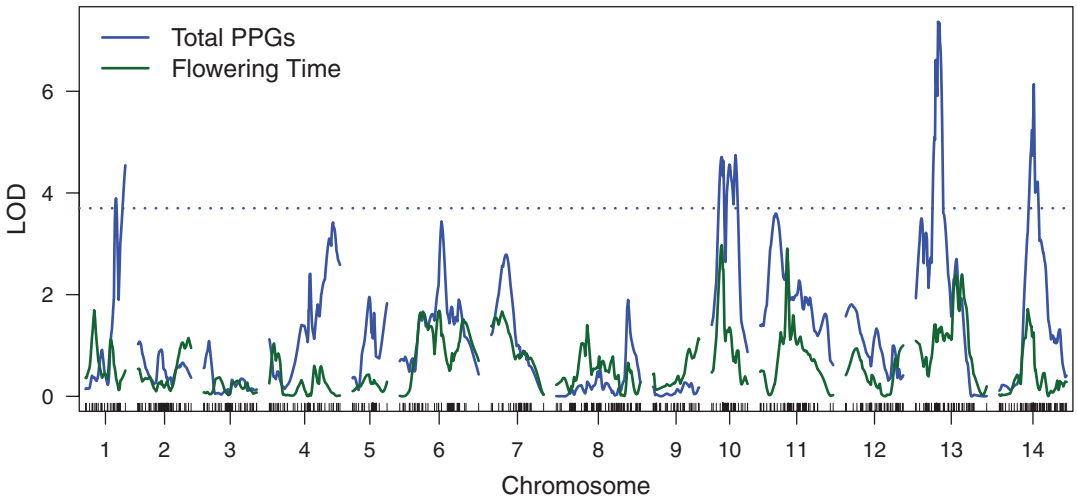

Figure 4. QTL map plotting of genome wide LOD scores for total PPGs (blue) and flowering time (green). Dotted line represents the statistical significance threshold determined via permutation test for the total PPGs analysis at $\alpha = 0.05$. The statistical significance threshold determined via permutation test for the flowering time analysis at $\alpha = 0.05$ was 3.78.

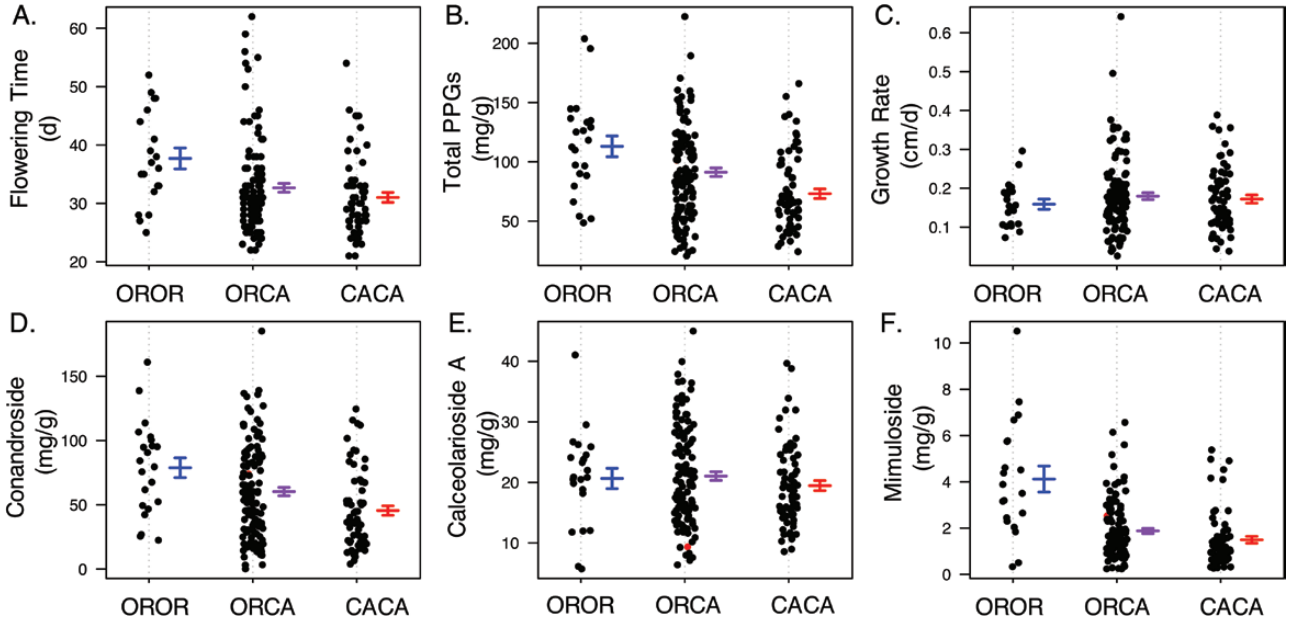

Figure 5. Phenotypic effects of the chromosome 10 QTL. The effects of allelic variation at marker 1662700 (window centered at 1 662 700 bp in the Mimulus IM62 V2 genome) on chr. 10 on (**A**) flowering time, (**B**) total PPGs, (**C**) growth rate, (**D**) conandroside, (**E**) calceolarioside A, and (**F**) mimuloside. This marker was the best estimate for QTLs associated with both flowering time and mimuloside and was within the 1.5 LOD support interval of all other collocated QTL. Every point is an individual in the F_2 mapping population, and hash markers represent the average and standard error within each genotype.

the abundances of individual PPGs, suggesting that pleiotropy or linkage of alleles causing variation in multiple traits contributes to the patterns of phenotypic correlation observed in nature (Figure 3). Total levels of PPGs and flowering time share only one QTL. However, this QTL has moderate to large effects relative to phenotypic differences between parental means, and the allelic effects are consistent with the direction of phenotypic differentiation between the parental lines (Figures 4 and 5). Pleiotropy or linkage also appears to play some role in the construction of PPG defense arsenals (Figures 5–7). Allelic variation at QTLs on chr. 13 and 14 is associated with increases in nearly all PPGs (Figures 6 and 7). However, the divergence in arsenals between parental plants also depends on several small- to moderate-effect QTLs that modify levels of individual PPGs that are spread across the genome (Figure 7). Below we discuss these results and their implications within the context of other genomic studies examining plant growth-defense trade-offs and evidence for pleiotropy in shaping patterns of diversity.

Genetic Basis of Trade-offs Between Growth/Reproduction and Levels of Defense

The phenotypic differences between parental lines largely matched population averages from our earlier population-level assessments of total PPG levels, PPG defense arsenals, and flowering time (Kooyers

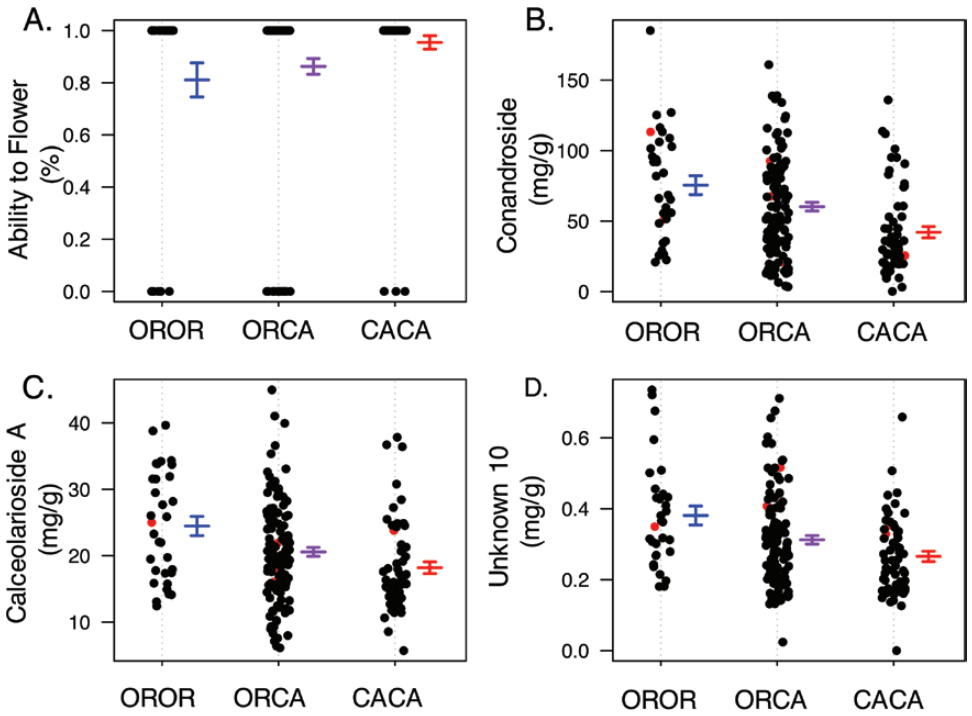

Figure 6. Phenotypic effects of the chromosome 14 QTL. The effects of allelic variation at marker 14297905 (window centered at 14 297 905 bp in the Mimulus IM62 V2 genome) on chr. 14 on (**A**) ability to flower, (**B**) conandroside, (**C**) calceolarioside A, and (**D**) unknown PPG 10. This marker was the best estimate for QTLs associated with both total PPGs and conandroside and was within the 1.5 LOD support interval for calceolarioside A and unknown PPG 10. This marker was ~1.5 Mbp outside of the 1.5 LOD support intervals for a QTL underlying the ability to flower. Every point is an individual in the F_2 mapping population. In the online version of this paper, black points are observed values and red points are inferred values for F_2 individuals with missing data at this marker. Hash markers represent the average and standard error within each genotype.

et al. 2017). The CA parental line grew faster, produced lower total levels of PPGs, and also produced a substantially different arsenal of PPGs (including higher calceolarioside A and lower conandroside levels) than the OR parental line, although the mean difference in total PPG levels was not as dramatic (Kooyers et al. 2017: CA 43.7 vs. OR 89.8 mg/g; current study: CA 71.5 vs. OR 82.0 mg/g). It is possible that inadvertent selection during the additional 1–2 generations of inbreeding that occurred between these 2 studies (and after F_1 production) may have reduced the differentiation. Notably, the variation in the F_2 generation exceeds both the parental lines in this experiment, recapturing the breadth of variation previously observed and thus making for an excellent genetic mapping resource.

The positive genetic correlations we observe between flowering time and constitutive defense levels suggest that increasing chemical defense production in annual monkeyflowers comes at the expense of allocating fewer resources toward rapid reproduction. Thus, adaptation to high herbivore pressure could impose a trade-off on achieving optimal reproduction timing, which is extremely important for annual plants that experience short growing seasons. Colocalizing QTLs for total PPG production and flowering time on chr. 10 (Figure 3) indicate that the correlation between total PPGs levels and flowering time is rooted in the genetic architecture of the variation in these traits. The allelic effects at this shared QTL matches expectations for a locus that controls allocation of resources to primary versus secondary metabolism; alleles that promote earlier flowering are associated with lower levels of constitutive defense. Results in other annual species suggest this may be widespread pattern. For example, a single locus underlies a trade-off between rapid development and herbivore resistance in *Cardamine hirsuta* (Rasmann et al. 2018). Determining whether trait relationships in *M. guttatus* stem from pleiotropy or close physical linkage of multiple loci will require determining the genetic basis of these phenotypes through fine mapping, assessment of candidate genes, and functional studies.

Growth rate and levels of total PPGs (Figure 3) were only weakly correlated in the F_2 mapping panel, suggesting little overlap in the loci that control defense and plant growth. Indeed, we did not detect any QTLs shared by total PPG levels and growth rate, and perhaps surprisingly, we did not find any significant QTLs for growth rate. Since there is reasonably high broad sense heritability in this trait, we expect the lack of detectable growth rate QTLs reflects a highly polygenic architecture with many loci of small effect underlying the difference observed between the parental lines, and we may have the power to detect these with a larger mapping population. The few other studies that have examined genetic correlations between growth and defense have reached mixed conclusions (Koricheva 2002; Züst and Agrawal 2017). For instance, *Oenothera biennis* has slightly positive genetic correlations between total phenolics and growth in roots and shoots (Parker et al. 2012), while *Asclepias syriaca* exhibits a negative genetic correlation between cardenolide concentration and growth rate (Züst et al. 2015). These mixed results in studies of genetic correlations do not necessarily suggest that costs of defense do not exist, but indicate that studies may need to assess growth and defensive traits in more detail (e.g., by tissue, developmental stage, environment, or type of defense) to determine how any such trade-offs manifest in different species (Züst and Agrawal 2017). One important factor may be accounting for maternal provisioning in calculating relative growth rate as has been demonstrated in *Arabidopsis* RIL lines (Paul-Victor et al. 2010).

Several recent studies have found trade-offs between growth and plant defense at the level of a single pleiotropic locus. In *Arabidopsis*,

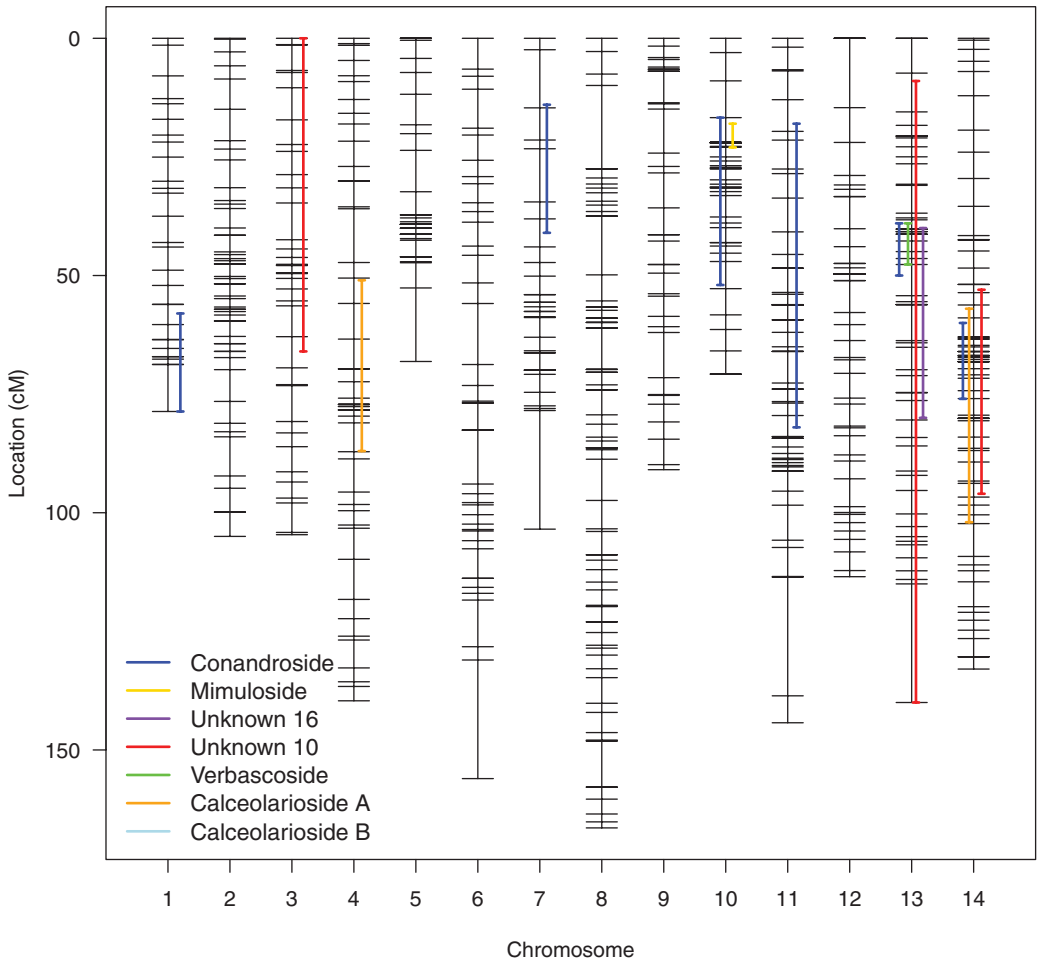

Figure 7. Genetic map for the CA × OR F_2 mapping population with QTL for different PPGs represented in different colors. The length of the line segments represents the 1.5 LOD support intervals for each QTL.

Todesco et al. (2010) find a single locus that has pleiotropic effects on plant defense and plant growth (as well as resistance to microbes). The allele conferring increased defense but slower growth segregates at intermediate frequencies throughout the range, suggesting that it does have some fitness advantage that allows persistence. Other studies in *Arabidopsis* have found trade-offs at loci between either growth rate and herbivory (Gloss et al. 2017) or flowering time and herbivore resistance (Weinig et al. 2003; Gloss et al. 2017). In these studies, differences in herbivory or herbivore resistance are measured rather than chemical defenses. Such differences in herbivory may be caused not only by an unmeasured plant defense but also by differences in plant apparency or differences in phenology.

Within our study species, work by Lowry et al. (2019) demonstrates that a trade-off between annual and perennial *M. guttatus* ecotypes exhibiting opposite patterns of growth, constitutive defense, and reproductive rate is associated with a single inversion polymorphism. This inversion stretches over hundreds of genes and suppresses recombination making it difficult to determine whether the observed phenotypic correlations are a product of pleiotropy or multiple linked genes. Notably, this inversion is in the "annual" orientation in both of our parental lines. However, the trade-offs between these annual and perennial ecotypes are analogous in some ways to those in our annual comparison, for example, rapid reproduction is associated with lower levels of PPGs. Despite the difference in study systems within *M. guttatus* (annual only vs. annual/perennial comparisons), both our study and Lowry et al.'s study suggest that pleiotropy or linkage underlies variation in total defense and reproductive rate, and thus genetic constraints may limit which phenotypic combinations may evolve, or how rapidly they can evolve, in nature.

Genetic Basis of Phytochemical Defense Arsenals

Divergence in the overall chemical defense levels and chemical defense arsenal appears to derive from segregating variation in at least 3 loci with effects shared across nearly all PPGs as well as several loci solely affecting individual defense metabolites. QTL analyses for almost all the PPGs detected moderate effect QTLs at overlapping regions of chr. 13 and 14 (Table 3) that are not significantly associated with growth or flowering time. Thus, these loci have pleiotropic effects on different chemical defense traits but do not necessarily affect resource allocation to primary metabolism. This result may be partly due to low power to detect an association between genotype and phenotype as there was a peak underlying variation in the ability to flower in the same region of chr. 14 that did not quite overlap with QTL (Figures 4 and 5); however, alternatively, the power gained from increased mapping panel size could also narrow LOD intervals. At the peak marker for the ability to flower QTL on chr. 14, the

OR allele is associated with higher concentration of all PPGs, which is consistent with the direction of the parental line difference for the majority of PPGs. That allelic variation could have pleiotropic impacts on all PPGs is not unexpected given that all PPGs share a biochemical precursor (Fraser and Chapple 2011; Keefover-Ring et al. 2014), and any mutation that alters enzymatic function or flow of metabolites in the shikimate or phenylpropanoid pathways prior to compounds diverting into the PPG biochemical pathway would affect levels of all PPGs. We thus might expect pleiotropy to be a major contributor to overall concentration with this closely related family of compounds (Berenbaum and Zangerl 1988; Zangerl and Berenbaum 1990).

While PPGs have some shared underlying genetic architecture, we also detected several small-effect QTL associated with variation in just 1 or 2 individual PPGs (Figure 6). These independent variants may contribute to the unique defense arsenals of the parental lines. For instance, the QTL on chr. 3 that is associated with variation in calceolarioside A and the QTL on chr. 4 that is associated with Unknown PPG 10 both do not overlap with any other QTLs. Each CA allele at the loci on chr. 3 and chr. 4 is associated with 23% or 36%, respectively, of the amount of divergence between the parental lines for levels of each of these 2 compounds, but these loci have little to no effect on the levels of the other PPGs (Supplementary Table S4). Notably, these 2 PPGs exhibited weaker correlations with other PPGs across populations in our previous study (Kooyers et al. 2017).

A previous QTL analysis in an annual × perennial *M. guttatus* cross-examining the genetic basis of PPGs found similar results with single, small-effect, independently segregating QTL underlying variation in 3 different PPGs (Holeski et al. 2014). A single QTL for Unknown PPG 16 on chr. 13 overlaps between that study and ours, but the effect sizes of this QTL in the annual × perennial cross accounted for less of the divergence between parental lines. These results suggest that a number of small to moderate effect genes control variation in related defense compounds to modify chemical arsenals rather than single QTLs associated with increases in some defense compounds but decreases in others (i.e., an "allocation" locus). This type of genetic architecture can lead to defense arsenals that are evolutionarily flexible, with the ability to respond to selection on individual compounds. Although few other studies have examined the genetic basis of variation in multiple closely related defense compounds, our results are not typical. In *Boechera stricta*, the proportion of methionine- versus branched-chain amino acid-derived glucosinolates is controlled by duplications and 2 nonsynonymous substitutions in the *BCMA* loci (Schranz et al. 2009; Prasad et al. 2012), limiting the evolutionary flexibility of this defense arsenal. The lack of "allocation" loci in our study may suggest that the causative mutations affects a gene upstream or at the base of the PPG branch of the phenylpropanoid pathway.

Conclusions

Here we find evidence that pleiotropy or genetic linkage may be important factors in producing some, but not all phenotypic correlations observed between defense and reproductive traits in natural populations. Colocalization of a single QTL between total PPGs and flowering time suggests pleiotropy or linkage contributes to correlations between these traits; however, this shared QTL explains a limited amount of variation in either trait. Because this level of genetic correlation alone is unlikely to explain fully the strong phenotypic correlations we have observed across natural populations between total PPGs and flowering time, we infer that correlational selection probably plays some role in generating these multivariate patterns. The presence of weak genetic correlations also suggests that there will be limited genetic constraint on future evolutionary responses. There may be a larger role for pleiotropy or close linkage in generating correlations between the concentrations of different PPGs as colocation of QTLs underlying the concentration of multiple PPGs is common. This may not be surprising as compounds that share a biochemical precursor are often highly correlated. While shared genetic architecture indicates that PPG arsenals have limited future evolutionary flexibility, there are a few QTLs that control levels of 1 or 2 PPGs each, suggesting some potential exists for fine-scale adaptation of defense arsenals to particular herbivore communities. Notably, the correlations between PPG concentrations in this single cross are similar to the correlations observed across the range of annual *M. guttatus* and thus may reflect widespread trade-offs. We anticipate that QTL mapping on a series of similar F_2 crosses within and between populations may corroborate this inference and reveal the extent and impact of genetic correlation, pleiotropy, and close linkage in generating range-wide patterns of phenotypic correlation.

Supplementary Material

Supplementary data are available at *Journal of Heredity* online.
Supplemental Figures and Tables
Fig. S1. Density plots for each PPG in the F_2 mapping population. Intervals for CA parent, OR parent and F_1 individuals are the standard deviation around the mean.
Table S1. Summary of morphological principal component analysis
Table S2. Sample sizes for QTL models for each phenotype
Table S3. Summary of chemistry and morphology principal component axes
Table S4. Summary statistics from the QTL analysis sorted by chromosome.
Table S5. Summary of multiple QTL models incorporating additive and epistatic effects.

Funding

This work was supported by the University of Louisiana, Lafayette, an Ecological, Evolutionary, and Conservation Genomics grant from the American Genetics Association to N.J.K., a New Research Grant from University of South Florida to N.J.K., a National Science Foundation grant (IOS-1558035) to N.J.K. and B.K.B., and a National Science Foundation grant (OIA-1920858) to N.J.K., and a Faculty Grants Program award from Northern Arizona University (L.M.H.).

Acknowledgments

We thank John K. Kelly for assistance developing and improving a linkage map, the University of South Florida Research Computing for access to their HPC cluster, the University of Central Florida Genomics Core for access to their PippenHT, and the Baker lab at USF for access to their lyophilizer. Constructive comments on this manuscript were provided by John Kelly and an anonymous reviewer.

Data Availability

The following files can be found on Dryad with DOI: https://doi.org/10.5061/dryad.w9ghx3fm8

Phenotype data in a .csv file
Raw sequencing reads in fastq. files
rQTL input in a .csv file

A custom perl script designed to group SNPs into 40bp windows can be found at https://github.com/BlackmanLabUCB/Genotyping-by-Sequencing

References

Andolfatto P, Davison D, Erezyilmaz D, Hu TT, Mast J, Sunayama-Morita T, Stern DL. 2011. Multiplexed shotgun genotyping for rapid and efficient genetic mapping. *Genome Res*. 21:610–617.

Arnold SJ. 1992. Constraints on phenotypic evolution. *Am Nat*. 140(Suppl (1):S85–107.

Berenbaum MR, Zangerl AR. 1988. Stalemates in the coevolutionary arms race: syntheses, synergisms, and sundry other sins. In: Kevin C. Spencer, editor. *Chemical mediation of coevolution*. San Diego (CA): Academic Press. p. 113–132.

Berenbaum MR, Zangerl AR. 1998. Chemical phenotype matching between a plant and its insect herbivore. *Proc Natl Acad Sci USA*. 95:13743–13748.

Brodie ED 3rd. 1992. Correlational selection for color pattern and antipredator behavior in the garter snake *Thamnophis ordinoides*. *Evolution*. 46:1284–1298.

Broman KW, Wu H, Sen S, Churchill GA. 2003. R/qtl: QTL mapping in experimental crosses. *Bioinformatics*. 19:889–890.

Carmona D, Lajeunesse MJ, Johnson MTJ. 2011. Plant traits that predict resistance to herbivores: traits that predict resistance to herbivores. *Funct Ecol*. 25:358–367.

Defossez E, Pellissier L, Rasmann S. 2018. The unfolding of plant growth form-defence syndromes along elevation gradients. *Ecol Lett*. 21:609–618.

Etterson JR, Shaw RG. 2001. Constraint to adaptive evolution in response to global warming. *Science*. 294:151–154.

Ferris KG, Barnett LL, Blackman BK, Willis JH. 2017. The genetic architecture of local adaptation and reproductive isolation in sympatry within the *Mimulus guttatus* species complex. *Mol Ecol*. 26:208–224.

Flagel LE, Blackman BK, Fishman L, Monnahan PJ, Sweigart A, Kelly JK. 2019. GOOGA: a platform to synthesize mapping experiments and identify genomic structural diversity. *PLoS Comput Biol*. 15:e1006949.

Flagel LE, Willis JH, Vision TJ. 2014. The standing pool of genomic structural variation in a natural population of *Mimulus guttatus*. *Genome Biol Evol*. 6:53–64.

Fraenkel GS. 1959. The raison d'ĕtre of secondary plant substances; these odd chemicals arose as a means of protecting plants from insects and now guide insects to food. *Science*. 129:1466–1470.

Fraser CM, Chapple C. 2011. The phenylpropanoid pathway in *Arabidopsis*. *Arabidopsis Book*. 9:e0152.

Friedman J, Twyford AD, Willis JH, Blackman BK. 2015. The extent and genetic basis of phenotypic divergence in life history traits in *Mimulus guttatus*. *Mol Ecol*. 24:111–122.

Gardner KM, Latta RG. 2007. Shared quantitative trait loci underlying the genetic correlation between continuous traits. *Mol Ecol*. 16:4195–4209.

Glaubitz JC, Casstevens TM, Lu F, Harriman J, Elshire RJ, Sun Q, Buckler ES. 2014. TASSEL-GBS: a high capacity genotyping by sequencing analysis pipeline. *PLoS One*. 9:e90346.

Gloss A, Brachi B, Feldmann M, Groen S, Bartoli C, Gouzy J, LaPlante E, Meyer C, Pyon H, Rogan S, *et al*. 2017. Genetic variants affecting plant size and chemical defenses jointly shape herbivory in *Arabidopsis*. *bioRxiv*. doi:10.1101/156299

Haley CS, Knott SA. 1992. A simple regression method for mapping quantitative trait loci in line crosses using flanking markers. *Heredity (Edinb)*. 69:315–324.

Hall MC, Willis JH. 2006. Divergent selection on flowering time contributes to local adaptation in *Mimulus guttatus* populations. *Evolution*. 60:2466–2477.

Hellsten U, Wright KM, Jenkins J, Shu S, Yuan Y, Wessler SR, Schmutz J, Willis JH, Rokhsar DS. 2013. Fine-scale variation in meiotic recombination in *Mimulus* inferred from population shotgun sequencing. *Proc Natl Acad Sci USA*. 110:19478–19482.

Herms DA, Mattson WJ. 1992. The dilemma of plants: to grow or defend. *Q Rev Biol*. 67:283–335.

Holeski LM. 2007. Within and between generation phenotypic plasticity in trichome density of *Mimulus guttatus*. *J Evol Biol*. 20:2092–2100.

Holeski LM, Hillstrom ML, Whitham TG, Lindroth RL. 2012. Relative importance of genetic, ontogenetic, induction, and seasonal variation in producing a multivariate defense phenotype in a foundation tree species. *Oecologia*. 170:695–707.

Holeski LM, Keefover-Ring K, Bowers MD, Harnenz ZT, Lindroth RL. 2013. Patterns of phytochemical variation in *Mimulus guttatus* (yellow monkeyflower). *J Chem Ecol*. 39:525–536.

Holeski LM, Monnahan P, Koseva B, McCool N, Lindroth RL, Kelly JK. 2014. A high-resolution genetic map of yellow monkeyflower identifies chemical defense QTLs and recombination rate variation. *G3 (Bethesda)*. 4:813–821.

Keefover-Ring K, Holeski LM, Bowers M, Clauss AD, Lindroth RL. 2014. Phenylpropanoid glycosides of *Mimulus guttatus* (yellow monkeyflower). *Phytochem Lett*. 10:132–139.

Kelly AJ, Willis JH. 1998. Polymorphic microsatellite loci in *Mimulus guttatus* and related species. *Mol Ecol*. 7:769–774.

Kooyers NJ, Blackman BK, Holeski LM. 2017. Optimal defense theory explains deviations from latitudinal herbivory defense hypothesis. *Ecology*. 98:1036–1048.

Kooyers NJ, Colicchio JM, Greenlee AB, Patterson E, Handloser NT, Blackman BK. 2019. Lagging adaptation to climate supersedes local adaptation to herbivory in an annual monkeyflower. *Am Nat*. 194:541–557.

Kooyers NJ, Greenlee AB, Colicchio JM, Oh M, Blackman BK. 2015. Replicate altitudinal clines reveal that evolutionary flexibility underlies adaptation to drought stress in annual *Mimulus guttatus*. *New Phytol*. 206:152–165.

Koricheva J. 2002. Meta-analysis of sources of variation in fitness costs of plant antiherbivore defenses. *Ecology*. 83:176–190.

Koricheva J, Nykänen H, Gianoli E. 2004. Meta-analysis of trade-offs among plant antiherbivore defenses: are plants jacks-of-all-trades, masters of all? *Am Nat*. 163:E64–E75.

Lande R. 1979. Quantitative genetic analysis of multivariate evolution, applied to brain:body size allometry. *Evolution*. 33:402–416.

Lander ES, Botstein D. 1989. Mapping mendelian factors underlying quantitative traits using RFLP linkage maps. *Genetics*. 121:185–199.

Langmead B, Salzberg SL. 2012. Fast gapped-read alignment with Bowtie 2. *Nat Methods*. 9:357–359.

Lowry DB, Popovic D, Brennan DJ, Holeski LM. 2019. Mechanisms of a locally adaptive shift in allocation among growth, reproduction, and herbivore resistance in *Mimulus guttatus*. *Evolution*. 73:1168–1181.

Lowry DB, Willis JH. 2010. A widespread chromosomal inversion polymorphism contributes to a major life-history transition, local adaptation, and reproductive isolation. *PLoS Biol*. 8:e1000500.

McGlothlin JW, Parker PG, Nolan V Jr, Ketterson ED. 2005. Correlational selection leads to genetic integration of body size and an attractive plumage trait in dark-eyed juncos. *Evolution*. 59:658–671.

McKay JK, Richards JH, Mitchell-Olds T. 2003. Genetics of drought adaptation in *Arabidopsis thaliana*: I. Pleiotropy contributes to genetic correlations among ecological traits. *Mol Ecol*. 12:1137–1151.

Mojica JP, Lee YW, Willis JH, Kelly JK. 2012. Spatially and temporally varying selection on intrapopulation quantitative trait loci for a life history trade-off in *Mimulus guttatus*. *Mol Ecol*. 21:3718–3728.

Molgaard P. 1986. Population genetics and geographical distribution of caffeic acid esters in leaves of *Plantago major* in Denmark. *J Ecol*. 74:1127.

Monnahan PJ, Kelly JK. 2017. The genomic architecture of flowering time varies across space and time in *Mimulus guttatus*. *Genetics*. 206:1621–1635.

Moore BD, Andrew RL, Külheim C, Foley WJ. 2014. Explaining intraspecific diversity in plant secondary metabolites in an ecological context. *New Phytol*. 201:733–750.

Nelson TC, Monnahan PJ, McIntosh MK, Anderson K, MacArthur-Waltz E, Finseth FR, Kelly JK, Fishman L. 2019. Extreme copy number vari-

ation at a tRNA ligase gene affecting phenology and fitness in yellow monkeyflowers. *Mol Ecol*. 28:1460–1475.

Paaby AB, Rockman MV. 2013. The many faces of pleiotropy. *Trends Genet*. 29:66–73.

Parker JD, Salminen JP, Agrawal AA. 2012. Evolutionary potential of root chemical defense: genetic correlations with shoot chemistry and plant growth. *J Chem Ecol*. 38:992–995.

Paul-Victor C, Züst T, Rees M, Kliebenstein DJ, Turnbull LA. 2010. A new method for measuring relative growth rate can uncover the costs of defensive compounds in *Arabidopsis thaliana*. *New Phytol*. 187:1102–1111.

Prasad KV, Song BH, Olson-Manning C, Anderson JT, Lee CR, Schranz ME, Windsor AJ, Clauss MJ, Manzaneda AJ, Naqvi I, *et al.* 2012. A gain-of-function polymorphism controlling complex traits and fitness in nature. *Science*. 337:1081–1084.

Puzey JR, Willis JH, Kelly JK. 2017. Population structure and local selection yield high genomic variation in *Mimulus guttatus*. *Mol Ecol*. 26:519–535.

Raguso RA, Agrawal AA, Douglas AE, Jander G, Kessler A, Poveda K, Thaler JS. 2015. The raison d'être of chemical ecology. *Ecology*. 96:617–630.

Rasmann S, Sánchez Vilas J, Glauser G, Cartolano M, Lempe J, Tsiantis M, Pannell JR. 2018. Pleiotropic effect of the *Flowering Locus C* on plant resistance and defence against insect herbivores. *Journal of Ecology*. 106:1244–1255.

Rotter MC, Couture JJ, Rothwell EM, Garcia J, Holeski LM. 2018. Evolutionary ecology of plant resistance traits across the herbivore diet spectrum: a test in the model plant *Mimulus guttatus*. *Evol Ecol Res*. 19:423–440.

Rotter MC, Vallejo-Marin M, Holeski LM. 2019. A test of the evolution of increased competitive ability in two invaded regions. *Evol Ecol*. 33:713–735.

Schranz ME, Manzaneda AJ, Windsor AJ, Clauss MJ, Mitchell-Olds T. 2009. Ecological genomics of *Boechera stricta*: identification of a QTL controlling the allocation of methionine- vs branched-chain amino acid-derived glucosinolates and levels of insect herbivory. *Heredity (Edinb)*. 102:465–474.

Stacklies W, Redestig H, Scholz M, Walther D, Selbig J. 2007. pcaMethods – a bioconductor package providing PCA methods for incomplete data. *Bioinformatics*. 23:1164–1167.

Stamp N. 2003. Out of the quagmire of plant defense hypotheses. *Q Rev Biol*. 78:23–55.

Stearns FW. 2010. One hundred years of pleiotropy: a retrospective. *Genetics*. 186:767–773.

Strauss SY, Rudgers JA, Lau JA, Irwin RE. 2002. Direct and ecological costs of resistance to herbivory. *Trends Ecol Evol*. 17:278–285.

Todesco M, Balasubramanian S, Hu TT, Traw MB, Horton M, Epple P, Kuhns C, Sureshkumar S, Schwartz C, Lanz C, *et al.* 2010. Natural allelic variation underlying a major fitness trade-off in *Arabidopsis thaliana*. *Nature*. 465:632–636.

Troth A, Puzey JR, Kim RS, Willis JH, Kelly JK. 2018. Selective trade-offs maintain alleles underpinning complex trait variation in plants. *Science*. 361:475–478.

Weinig C, Stinchcombe JR, Schmitt J. 2003. QTL architecture of resistance and tolerance traits in *Arabidopsis thaliana* in natural environments. *Mol Ecol*. 12:1153–1163.

Wu CA, Lowry DB, Cooley AM, Wright KM, Lee YW, Willis JH. 2008. Mimulus is an emerging model system for the integration of ecological and genomic studies. *Heredity (Edinb)*. 100:220–230.

Zangerl AR, Berenbaum MR. 1990. Furanocoumarin induction in wild parsnip: genetics and population variation. *Ecology*. 71:1933–1940.

Züst T, Agrawal AA. 2017. Trade-offs between plant growth and defense against insect herbivory: an emerging mechanistic synthesis. *Annu Rev Plant Biol*. 68:513–534.

Züst, T, Rasmann S, Agrawal AA. 2015. Growth-defense tradeoffs for two major anti-herbivore traits of the common milkweed *Asclepias syriaca*. *Oikos*. 124:1404–1415.

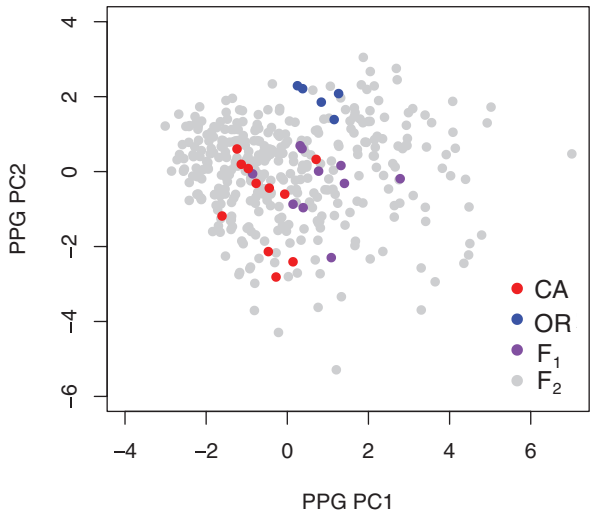

Figure 2

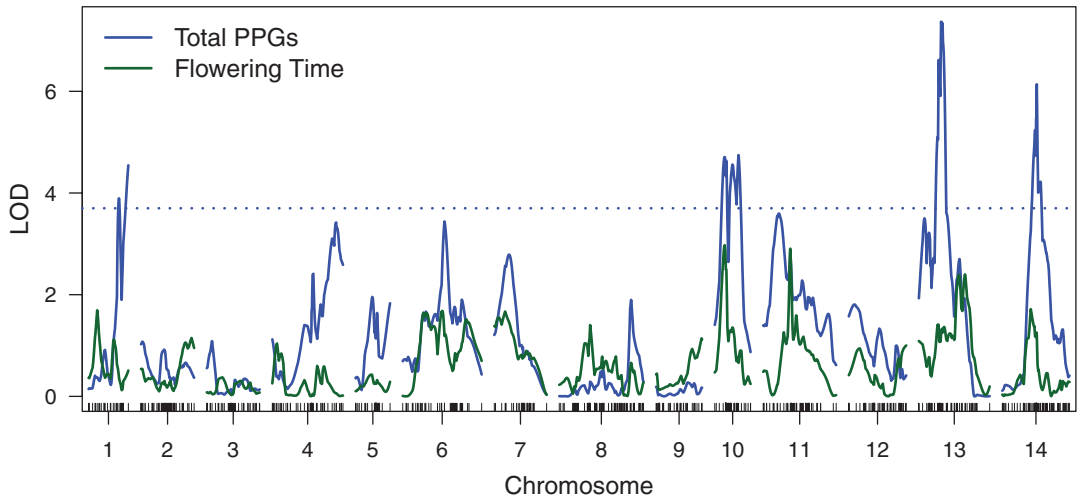

Figure 4

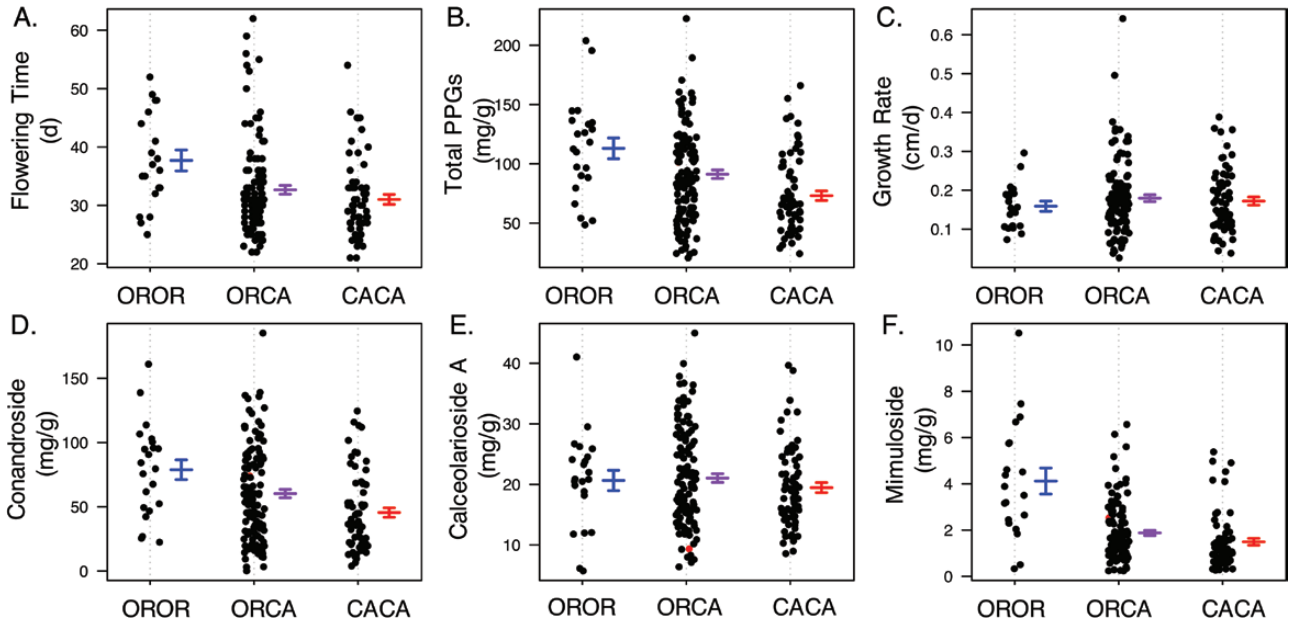

Figure 5

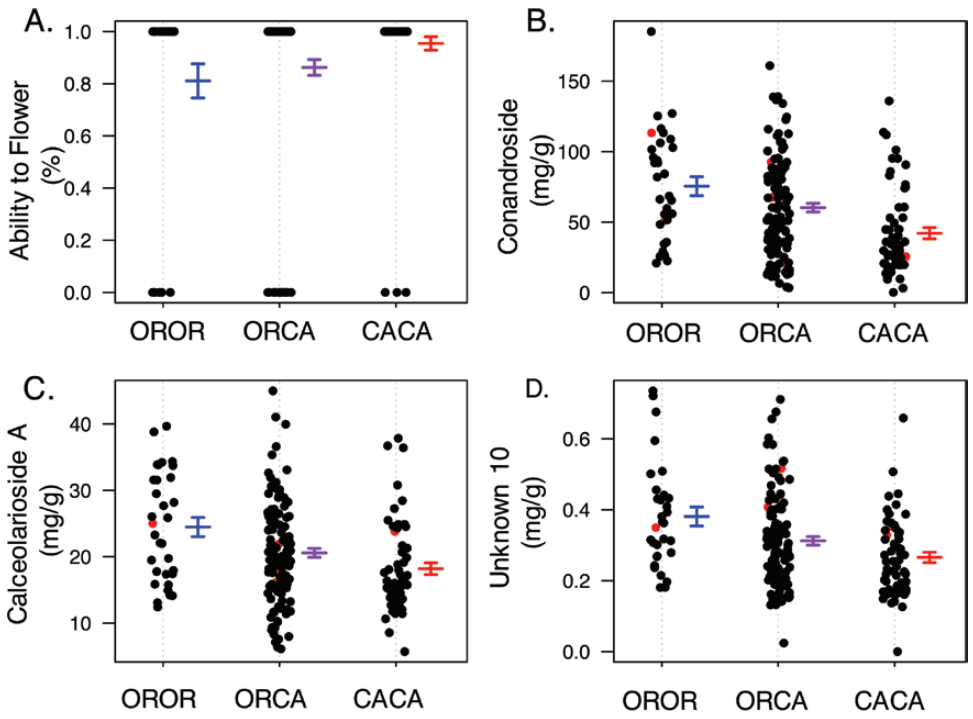

Figure 6

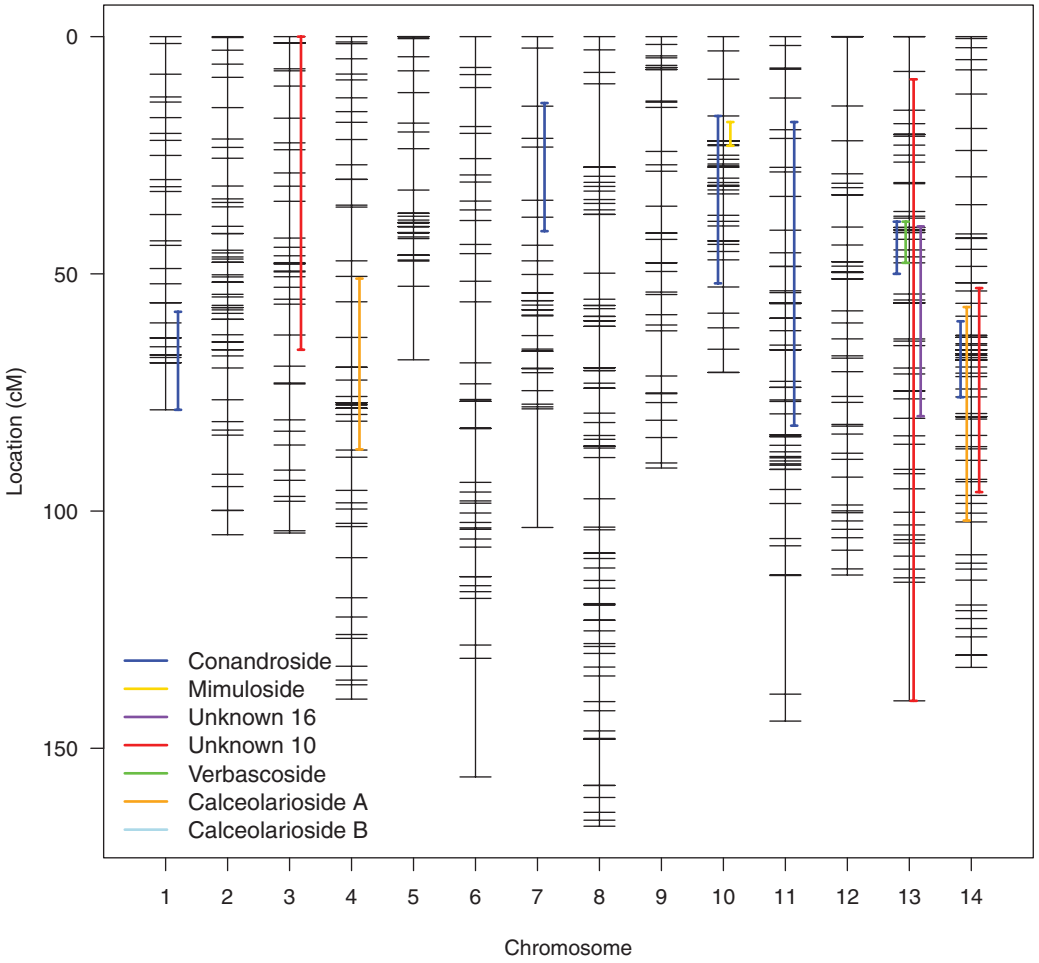

Figure 7